Supporting information

Graphene Oxide-Grafted Magnetic Nanorings Mediated Magnetothermodynamic Therapy Favoring Reactive Oxygen Species-Related Immune Response for Enhanced Antitumor Efficacy

*Xiaoli Liu,[†,‡,⊥] Bin Yan,[†,⊥] Yao Li,[‡] Xiaowei Ma,[‡] Wangbo Jiao,[§] Kejian Shi,[Δ] Tingbin Zhang,[§] Shizhu Chen,[∥,∇] Yuan He,[§] Xing-Jie Liang,[‡] and Haiming Fan[†,§,]**

† Key Laboratory of Resource Biology and Biotechnology in Western China, Ministry of Education; School of Medicine, Northwest University, 229 Taibai North Road, Xi'an 710069, China.

§ Key Laboratory of Synthetic and Natural Functional Molecule Chemistry of the Ministry of Education, College of Chemistry and Materials Science, Northwest University, Xi'an 710127, China

‡ CAS Key Laboratory for Biomedical Effects of Nanomaterials and Nanosafety, CAS Center for Excellence in Nanoscience, National Center for Nanoscience and Technology of China, No. 11, First North Road, Zhongguancun, Beijing 100190, China
University of Chinese Academy of Sciences, Beijing 100049, China

Δ Beijing Institute of Traumatology and Orthopaedics, Beijing 100035, China

∥ Beijing General Pharmaceutical Corporation, Beijing 100101, China

∇ The National Institutes of Pharmaceutical R&D Co., Ltd., China Resources Pharmaceutical Group Limited, Beijing 102206, China

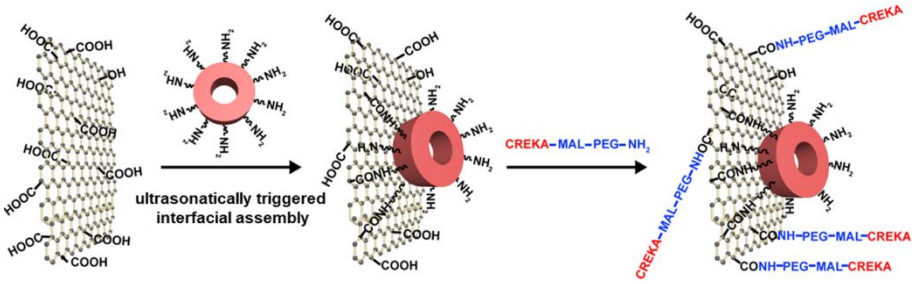

Figure S1. Schematic illustration of FVIOs-GO preparation process.

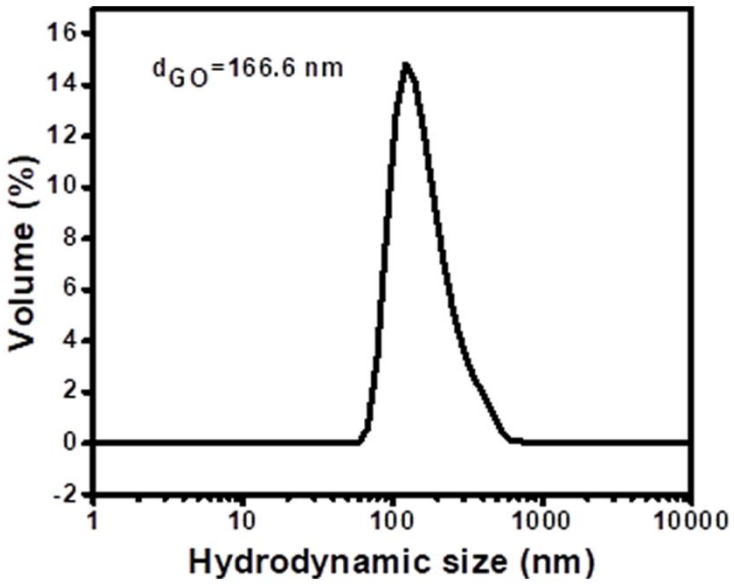

Figure S2. Hydrodynamic size of GO nanosheets.

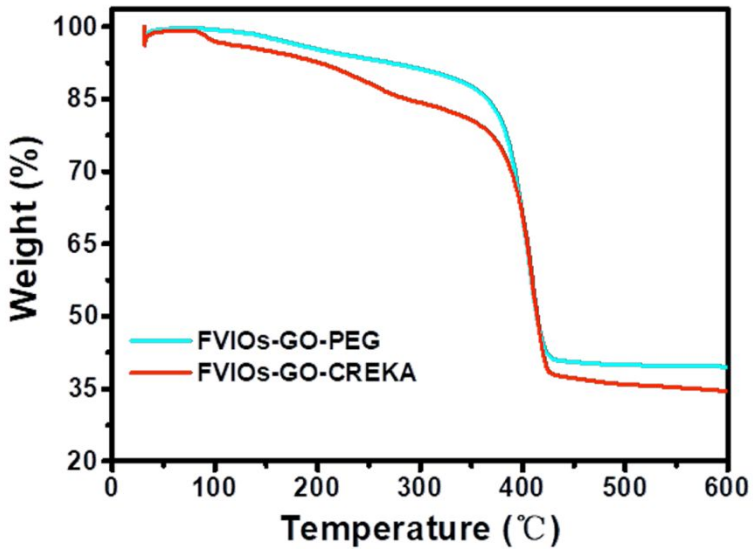

Figure S3. TGA curves of FVIOs-GO-PEG and FVIOs-GO-CREKA.

Table S1. Summary of several parameters, including SAR and ILP values of MNPs.

	Core size (nm)	Shape	*H* (kA/m)	*f* (kHz)	SAR (W/g)	ILP (nHm^2/kg)	Reference
FVIOs-GO	70	Rings	31.2	365	2570	7.27	This study
FVIOs-PEG	70	Rings	32.4	365	1319	3.46	This study
FVIOs	70	Rings	35	400	2213	4.52	[1]
Resovist		Spherical	35	400	104	0.21	[1]
Fe_3O_4	43	Octahedral	63	358	2483	1.75	[2]
Fe_3O_4	19	Cubic	29	520	2452	5.60	[3]
CoMn-Fe_3O_4	14.8	Hexagon	26.9	420	1718.0	5.65	[4]
$CoFe_2O_4$@$MnFe_2O_4$	15	Core-shell	37.3	500	2250	3.23	[5]
Fe_3O_4	33	Clusters	23.8	302	253	1.48	[6]
Fe_3O_4	19	Spherical	27	400	535	1.83	[7]

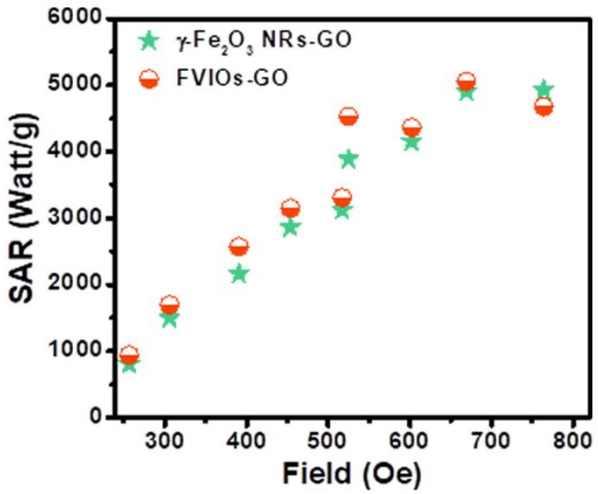

Figure S4. SAR of γ-Fe_2O_3 NRs-GO and FVIOs-GO.

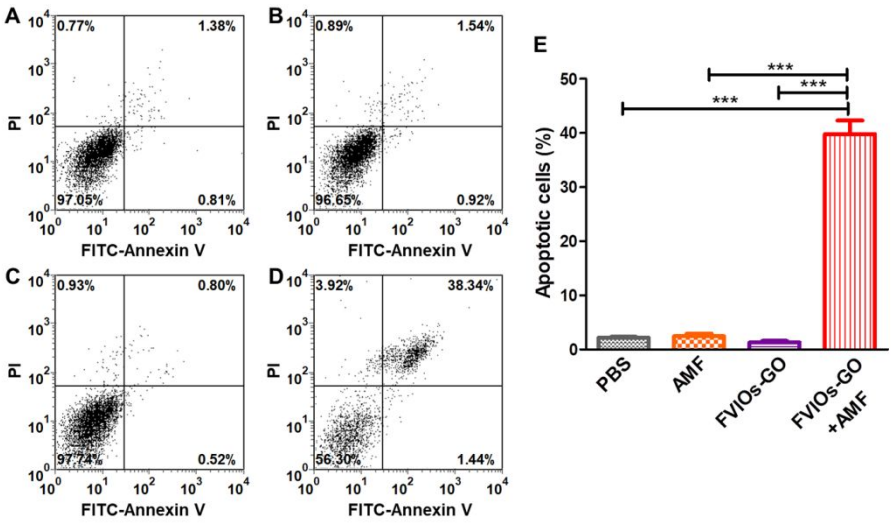

Figure S5. (A)-(D) Flow cytometry analysis and (E) quantification of apoptosis and/or necrosis of 4T1 tumor cells after various treatment. 4T1 cells were treated with FVIOs-GO at a Fe concentration of 50 μg/mL, and were subsequently exposed to AMF (365 kHz, 400 Oe) for 10 min. The One-way ANOVA with Tukey's multiple comparison tests was used to analyses differences among the groups. Data are reported as mean values ±SEM. P value <0.05 was considered statistically significant, and the number of the label "*" represents the range of P values (*0.01 < P < 0.05; **0.001 < P < 0.01; ***P < 0.001).

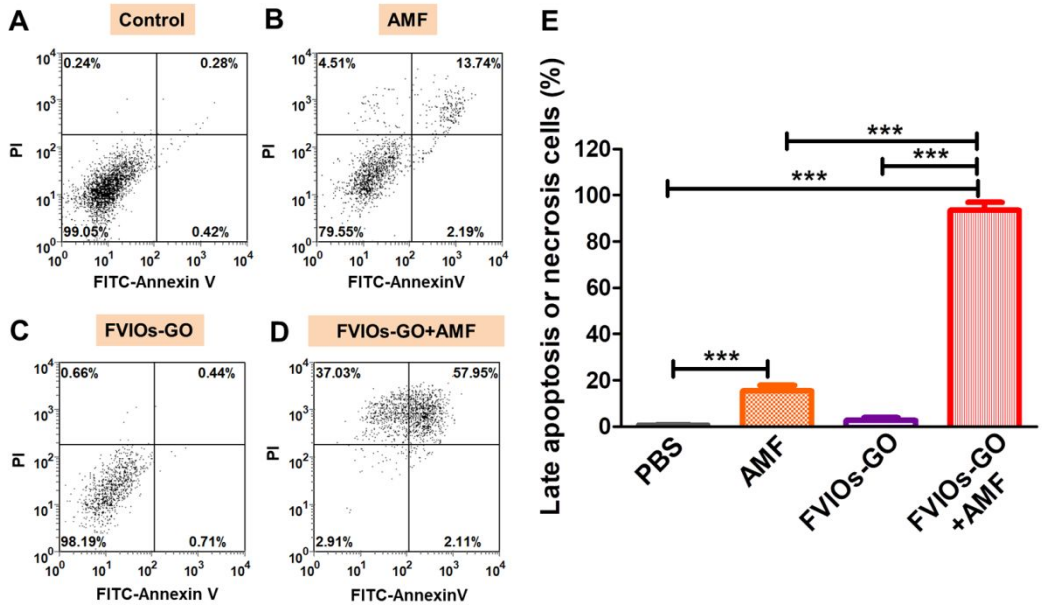

Figure S6. (A)-(D) Flow cytometry analysis and (E) quantification of apoptosis and/or necrosis of 4T1 tumor cells after various treatment. 4T1 cells were treated with FVIOs-GO at a Fe concentration of 75 μg/mL, and were subsequently exposed to AMF for 15 min. The One-way ANOVA with Tukey's multiple comparison tests was used to analyses differences among the groups. Data are reported as mean values ±SEM. P value <0.05 was considered statistically significant, and the number of the label "*" represents the range of P values (*0.01 < P < 0.05; **0.001 < P < 0.01; ***P < 0.001).

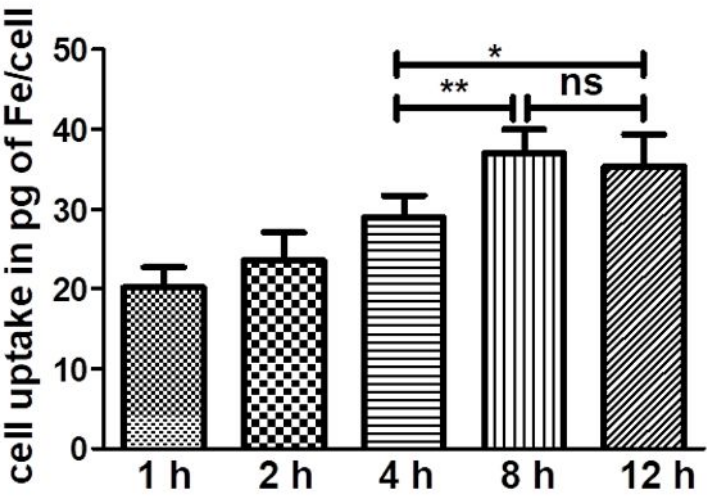

Figure S7. Quantitative study of cellular uptake efficiency of FVIOs-GO-CREKA after 1 h, 2 h, 4 h, 8 h, and 12 h incubation, respectively. The One-way ANOVA with Tukey's multiple comparison tests was used to analyses differences among the groups. Data are reported as mean values ±SEM. P value <0.05 was considered statistically significant, and the number of the label "*" represents the range of P values (*0.01 < P < 0.05; **0.001 < P < 0.01; ***P < 0.001).

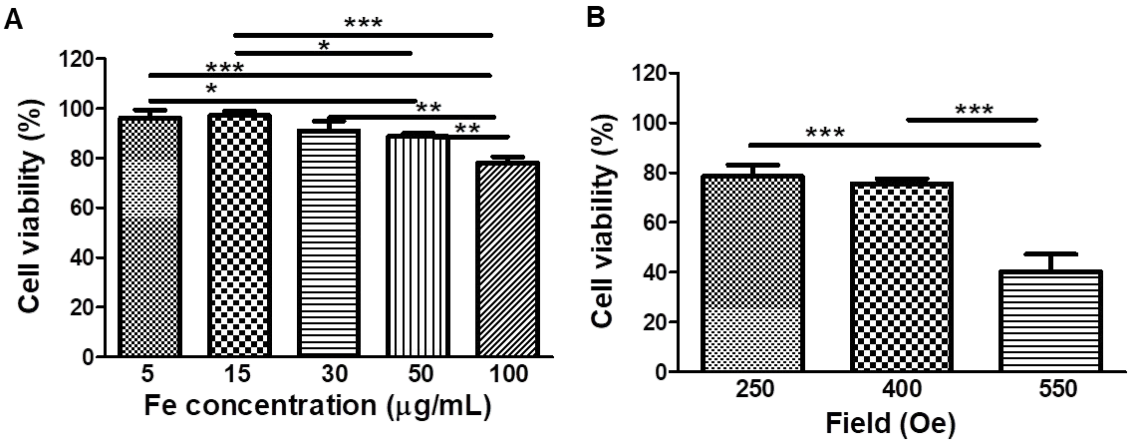

Figure S8. (A) Cell viability of RAW264.7 cells after 24 h incubation with FVIOs-GO. (B) Cell viability of RAW264.7 cells after treatment by FVIOs-GO + AMF with different field. The One-way ANOVA with Tukey's multiple comparison tests was used to analyses differences among the groups. Data are

reported as mean values ±SEM. P value <0.05 was considered statistically significant, and the number of the label "*" represents the range of P values (*0.01 < P < 0.05; **0.001 < P < 0.01; ***P < 0.001).

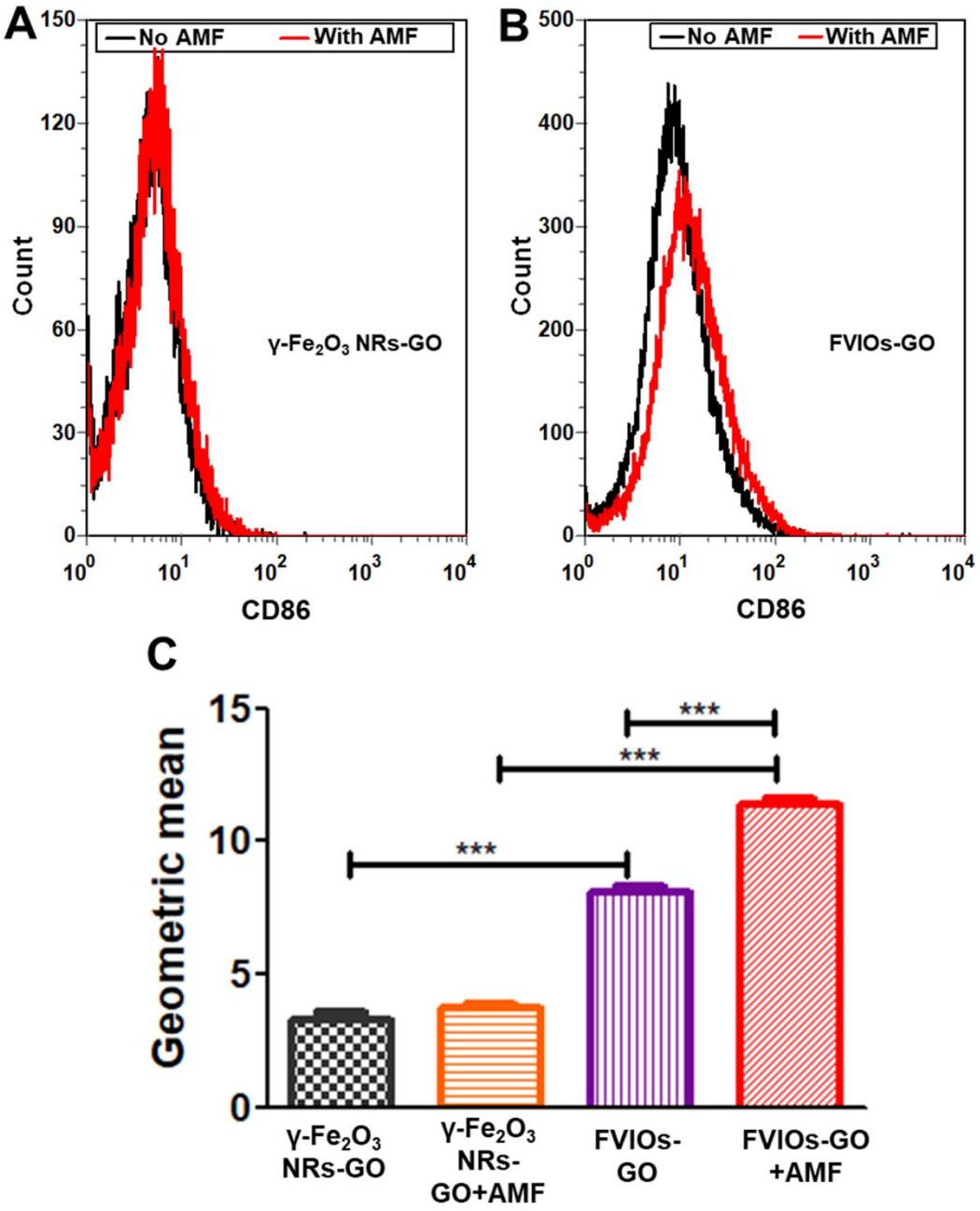

Figure S9. (A)-(B) Flow cytometry of phenotypes of macrophages (RAW264.7) after with different treatment. (C) Quantification of M1 macrophages. The One-way ANOVA with Tukey's multiple comparison tests was used to analyses differences among the groups. Data are reported as mean values ±SD. P value <0.05 was considered statistically significant, and the number of the label "*" represents the range of P values (*0.01 < P < 0.05; **0.001 < P < 0.01; ***P < 0.001).

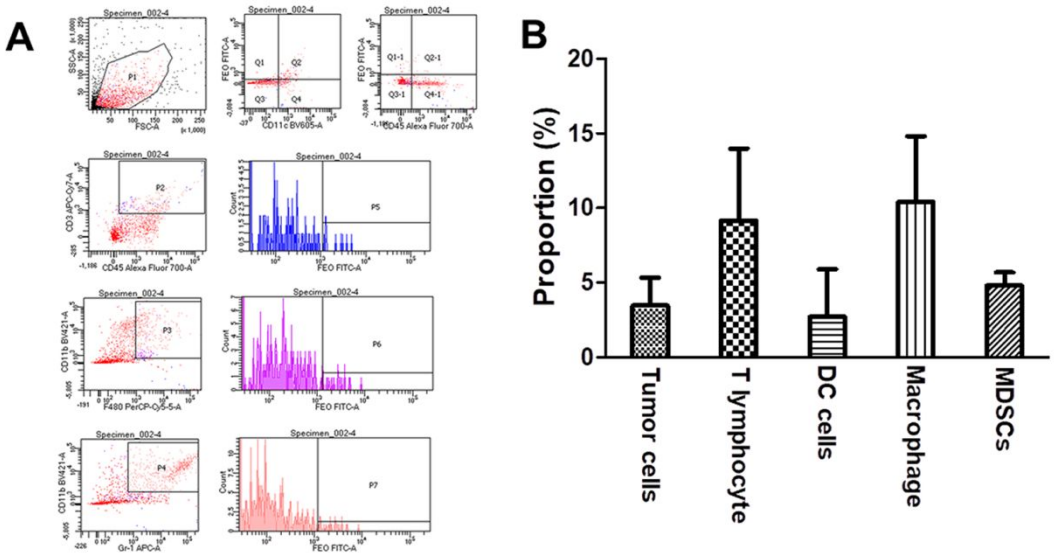

Figure S10. Analyzing which cells in the tumor take up the FVIOs-GO and on the distribution of FVIOs-GO in the 4T1 tumor, FITC-labeled FVIOs-GO directly injected into tumors (3 mice per group), after 24 h, the tumors were harvested from the mice and digested. The percentages of tumor cells (CD 45^-), T lymphocyte ($CD45^+CD3^+$), DC cells (CD $11c^+$), macrophage (CD $11b^+F4/80^+$) and MDSCs ($CD11b^+Gr\text{-}1^+$) in the total cells for taking up FITC-labeled FVIOs-GO were analyzed by flow cytometry analysis.

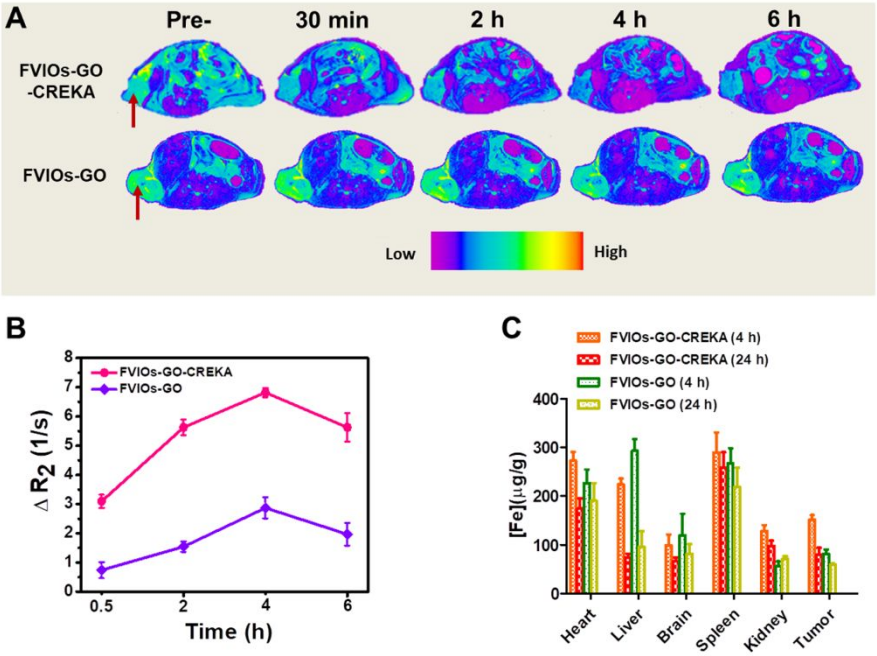

Figure S11. (A) T_2-weighted MR images acquired at different time points after intravenous administration of FVIOs-GO-CREKA or FVIOs-GO in the subcutaneous 4T1 breast tumor-bearing mice ($C_{[Fe]}$ = 3.0 mg/kg). (B) Δ R_2 value of tumor after intravenous injection of FVIOs-GO-CREKA or FVIOs-GO at 30 min, 2 h, 4 h and 6 h post injection. (C) Biodistribution and tumor uptake of FVIOs-GO-CREKA or FVIOs-GO in 4T1 tumor-bearing mice.

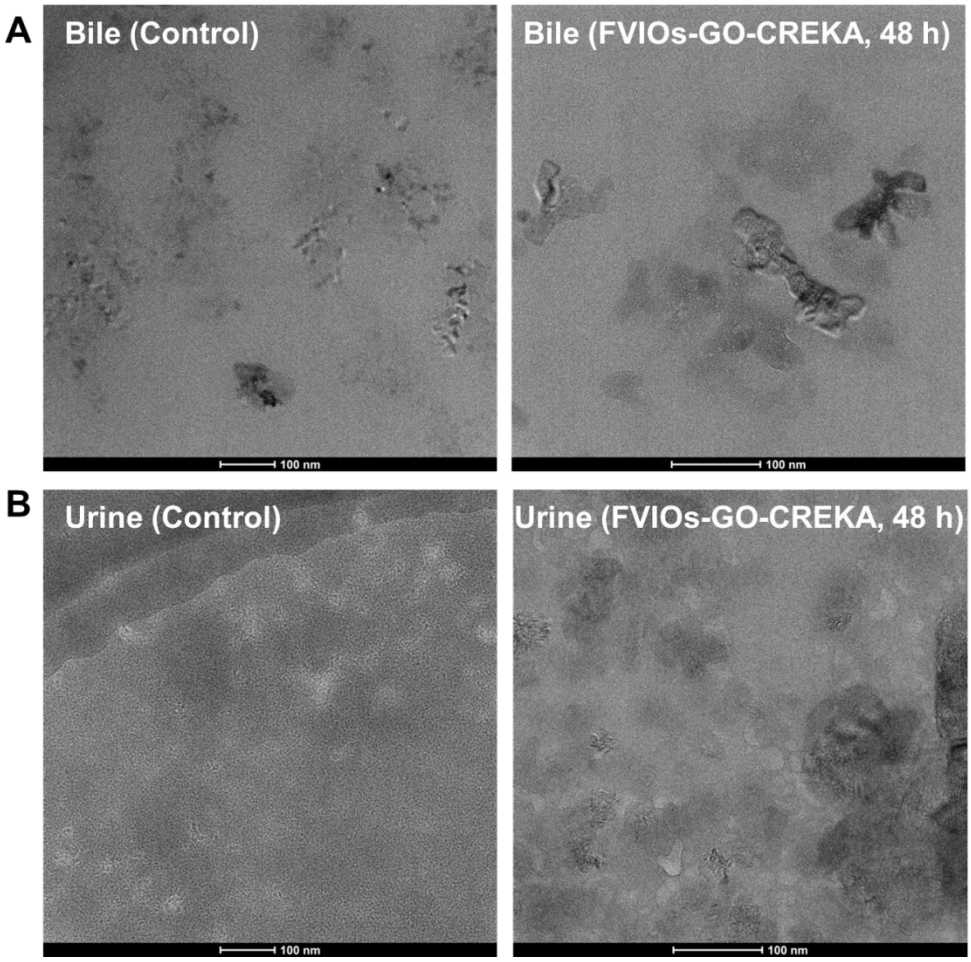

Figure S12. (A) TEM images for bile before and post injection FVIOs-GO-CREKA. (B) TEM images for urine before and post injection FVIOs-GO-CREKA.

REFERENCES

(1) Liu, X. L.; Yang, Y.; Ng, C. T.; Zhao, L. Y.; Zhang, Y.; Bay, B. H.; Fan, H. M.; Ding, J. Magnetic Vortex Nanorings: A New Class of Hyperthermia Agent for Highly Efficient *In Vivo* Regression of Tumors. *Adv. Mater.* **2015,** *27*, 1939-1944.

(2) Lv, Y.; Yang, Y.; Fang, J.; Zhang, H.; Peng, E.; Liu, X.; Xiao, W.; Ding, J. Size Dependent Magnetic Hyperthermia of Octahedral Fe_3O_4 Nanoparticles. *RSC Adv.* **2015,** *5*, 76764-76771.

(3) Guardia, P.; Di Corato, R.; Lartigue, L.; Wilhelm, C.; Espinosa, A.; Garcia-Hernandez, M.; Gazeau, F.; Manna, L.; Pellegrino, T. Water-Soluble Iron Oxide Nanocubes with High Values of Specific Absorption Rate for Cancer Cell Hyperthermia Treatment. *ACS Nano* **2012,** *6*, 3080-3091.

(4) Albarqi, H. A.; Wong, L. H.; Schumann, C.; Sabei, F. Y.; Korzun, T.; Li, X. N.; Hansen, M. N.; Dhagat, P.; Moses, A. S.; Taratula, O. Biocompatible Nanoclusters with High Heating Efficiency for Systemically Delivered Magnetic Hyperthermia. *ACS Nano* **2019,** *13*, 6383-6395.

(5) Lee, J. H.; Jang, J. T.; Choi, J. S.; Moon, S. H.; Noh, S. H.; Kim, J. W.; Kim, J. G.; Kim, I. S.; Park, K. I.; Cheon, J. Exchange-Coupled Magnetic Nanoparticles for Efficient Heat Induction. *Nat. Nanotechnol.* **2011,** *6*, 418-422.

(6) Niculaes, D.; Lak, A.; Anyfantis, G. C.; Marras, S.; Laslett, O.; Avugadda, S. K.; Cassani, M.; Serantes, D.; Hovorka, O.; Chantrell, R.; Pellegrino, T. Asymmetric Assembling of Iron Oxide Nanocubes for Improving Magnetic Hyperthermia Performance. *ACS Nano* **2017,** *11*, 12121-12133.

(7) Liu, X. L.; Fan, H. M.; Yi, J. B.; Yang, Y.; Choo, E. S. G.; Xue, J. M.; Di Fan, D.; Ding, J. Optimization of Surface Coating on Fe_3O_4 Nanoparticles for High Performance Magnetic Hyperthermia Agents. *J. Mater. Chem.* **2012,** *22*, 8235-8244.